ELSEVIER

Contents lists available at ScienceDirect

#### Construction and Building Materials

journal homepage: www.elsevier.com/locate/conbuildmat



### Numerical service-life modeling of chloride-induced corrosion in recycled-aggregate concrete



Nathan D. Stambaugh, Todd L. Bergman, Wil V. Srubar III\*

Department of Civil, Environmental, and Architectural Engineering, University of Colorado Boulder, ECOT 441 UCB 428, Boulder, CO 80309-0428, USA

#### HIGHLIGHTS

- We present a 1D numerical service-life model for recycled aggregate (RA) concrete.
- The model accounts for both normal and chloride-contaminated RAs.
- RA concretes modeled herein ranged in service life from  $\sim$ 10 to 80 years.
- Location and exposure conditions most affect service life in chloride environments.
- In design, moderate to high RA content and some contamination may be acceptable.

#### ARTICLE INFO

## Article history: Received 10 July 2017 Received in revised form 15 November 2017 Accepted 17 November 2017 Available online 6 December 2017

# Keywords: Recycled aggregate concrete Supplementary cementitious materials Service-life prediction Chloride-induced corrosion Numerical modeling

#### ABSTRACT

This paper presents the theoretical development, validation, and implementation of a 1D numerical service-life prediction model for reinforced recycled aggregate concrete exposed to internal and external sources of chlorides. The model accounts for the inclusion of supplementary cementitious materials (SCMs), namely (a) fly ash, (b) slag, (c) silica fume, and (d) metakaolin, and recycled aggregates (i) with and (ii) without initial chloride contamination from previous in-service exposure. The model is used to predict time to corrosion-induced cracking for reinforced recycled aggregate concrete in five casestudy applications, namely structures in a marine splash zone (Zone I), a marine spray zone (Zone II), within 800 km of coastline (Zone III), within 1.5 km of coastline (Zone IV), and parking structures at locations greater than 1.5 km from the coastline (Zone V) in Los Angeles, California and Anchorage, Alaska. The effects of recycled aggregate size, aggregate replacement ratio, degree of aggregate precontamination, water-to-cement (w/c) ratio, and SCMs on time-to-cracking of reinforced recycled aggregate concrete are elucidated herein. The potential for SCMs to improve the service life of recycled aggregate concrete is investigated by estimating additions required to meet a target service life of 50 years. Results indicate that, in addition to geographic location, temperature, and severity of exposure, w/c ratio and aggregate replacement ratio exhibit the greatest impact on time to chloride-induced cracking in reinforced recycled aggregate concrete. Furthermore, initial aggregate chloride contamination and aggregate size impart minimal effects on expected service life. Finally, the results illustrate that the use of either fly ash or slag is most viable in achieving a 50-year service life for the recycled aggregate concretes in chloride-laden environments considered in this work.

© 2017 Elsevier Ltd. All rights reserved.

#### 1. Introduction

Worldwide, concrete is the most common building material and the second most consumed material on Earth after water [1]. Subsequently, its production, use, and disposal have global environmental consequences. The production of cement alone is

\* Corresponding author.

E-mail address: wsrubar@colorado.edu (W.V. Srubar III).

responsible for 5–8% of anthropogenic carbon dioxide emissions, which exacerbates effects related to global warming and climate change [2]. In addition, debris generated by the demolition of concrete structures is a large contributor to industrial waste streams. While using recycled concrete in low-performance applications is a common practice, the use of crushed recycled concrete as aggregate in new structural concrete remains uncommon, primarily due to a lack of confidence in mechanical properties [3,4] and appropriate modeling tools to predict long-term performance.

#### 1.1. Service-life prediction of recycled aggregate concrete

Chloride-induced corrosion is one of the most common durability issues encountered by reinforced concrete structures. Laboratory and modeling studies have consistently shown that the chloride permeability of recycled aggregate concrete increases with aggregate replacement ratio due to increases in average pore size and total concrete porosity [5–9]. Other experimental studies have shown that chloride resistance can be further compromised by initial contamination of recycled aggregates from previous inservice exposure [10,11].

To improve confidence in the long-term durability of both normal and recycled aggregate concrete, engineers require suitable modeling tools to estimate the service-life performance of concrete structures in chloride-laden environments. Despite being widely used, service-life prediction tools, such as Life-365™ [12] and STA-DIUM<sup>®</sup> [13], do not yet account for the use of recycled aggregates. However, several researchers have proposed models to predict chloride transport in recycled aggregate concrete, including the authors, who previously proposed the first steady-state model for chloride diffusion in both contaminated- and non-contaminated recycled aggregate concrete. Xiao, et al. [14] used the finite element method to conduct a parametric study that elucidated the effects of aggregate replacement ratio, shape, boundary conditions, and attached mortar on the effective diffusivity of recycled aggregate concrete. Ying, et al. [15] proposed a new model that described the effects of recycled aggregate distribution on chloride diffusion. Srubar [11] proposed a steady-state 1D solution to Fick's Second Law of Diffusion that accounted for pre-contamination of recycled aggregates. The model was based on dopant-diffusion principles in which a substrate is doped with concentrations of another material that diffuse throughout the bulk over time. Despite this modeling advance for contaminated recycled aggregate concrete, incapability of accounting for non-steady-state boundary conditions and time-dependent changes in the chloride diffusion coefficient is a limitation of the approach.

#### 1.2. Scope of work

To address the limitations of the previously proposed steadystate chloride diffusion model for reinforced recycled aggregate concrete, this paper presents the formulation, validation, and implementation of a 1D numerical finite difference solution to Fick's Second Law of Diffusion that is used with a simplified cracking model to predict time to corrosion-induced cracking in contaminated and non-contaminated recycled aggregate concrete. The model, which is based on the finite difference solution employed in Life-365<sup>™</sup> [12], accounts for non-steady-state chloride boundary conditions, recycled aggregate size, placement, replacement ratio, and initial degree of contamination, and effects of water-to-cement (w/c) ratio, time, temperature, and supplementary cementitious material (SCM) additions on the chloride diffusion coefficient. The numerical model is first validated with Life-365™ using normal aggregate concrete and is subsequently enhanced with the most current parametric relationships and implemented using a stochastic approach to estimate time to corrosion-induced cracking of recycled aggregate concrete in five case-study applications, namely structures in a marine splash zone (Zone I), a marine spray zone (Zone II), within 800 km of coastline (Zone III), within 1.5 km of coastline (Zone IV) and parking structures (Zone V) in Los Angeles, California and Anchorage, Alaska. In addition to elucidating the effects of key modeling parameters, the amount and type of SCM required to meet a target service life of 50 years in each case-study application is investigated herein.

#### 2. Model development

The time to corrosion-induced cracking was estimated using a two-part damage model first proposed by Tuutti [16]. The model considers the total service life,  $t_s$ , of reinforced recycled aggregate concrete the sum of two successive time periods, namely, time to corrosion initiation,  $t_i$ , which is governed by the diffusion of chlorides throughout the concrete media, and the time to corrosion cracking,  $t_c$ .

#### 2.1. Time to corrosion initiation

Time to corrosion initiation is a function of the transport properties of the concrete, geometry, the boundary conditions that exist for a given environment and application, and the required concentration of chlorides to initiate the corrosion of the reinforcing steel (i.e., chloride threshold). Corrosion initiation is defined as the time that it takes for chlorides from the surrounding environment to penetrate the concrete cover and accumulate to a sufficient concentration at the reinforcement surface to initiate corrosion. Chloride concentrations above the chloride threshold locally reduce the pH near the reinforcement, which results in depassivation of the protective oxide layer and subsequent corrosion of the steel reinforcement.

Chloride transport can take place due to a number of mechanisms including (a) diffusion under the influence of a concentration gradient, (b) absorption due to capillary action, (c) migration in an electrical field, and (d) pressure-induced flow and wick action when water absorption and water vapor diffusion are combined [17]. Ionic diffusion of chloride is the primary mechanism of chloride transport and is considered the sole mechanism for the models discussed in this study. It has been shown that the relationship between chloride concentration, diffusion coefficient, and time in the random molecular motions of chloride ions in concrete can be described using Fick's Second Law of Diffusion [18], a governing second-order partial differential equation that is used to characterize the diffusion process:

$$\frac{\partial C}{\partial t} = -D \frac{\partial^2 C}{\partial x^2} \tag{1}$$

where C is the chloride concentration (kg/m<sup>3</sup>), D is the apparent diffusion coefficient (m<sup>2</sup>/s), x is the depth from the exposed concrete surface (m), and t is time (s).

A finite difference method is employed to numerically solve the diffusion equation and estimate time to corrosion initiation. The approach is based on the well-known Life-365™ service-life prediction software [12], which utilizes the Crank-Nicolson finite difference method to numerically solve the diffusion equation for normal aggregate concrete. The Crank-Nicolson approach is implemented here to account for limitations of the simple error function solution previously reported by the authors [11], namely its inabilities to account for non-steady state boundary conditions and time-dependent changes in chloride diffusion coefficients.

According to the method, a 1D representation of the concrete cover depth is divided into a finite number of slices, s, and nodes, n, where n = s + 1. The chloride concentration at an arbitrary node, i, at a timestep of t + 1 is calculated by the advection-dispersion equation:

$$-ru_{i+1}^{t+1} + (1+2r)u_i^{t+1} - ru_{i-1}^{t+1} = ru_{i+1}^t + (1-2r)u_i^t + ru_{i-1}^t$$
 (2)

where the dimensionless Courant-Friedrichs-Lewy (CFL) number:

$$r = D_{t,T} \left( \frac{dt}{2(dx)^2} \right) \tag{3}$$

and where  $D_{t,T}$  is the diffusion coefficient (m²/s) at time, t, and temperature, T,  $d_t$  is the timestep (s), dx is the length of each slice (m), and  $u_t^t$  is the chloride concentration (kg/m³) at the node at time, t. The left side of Eq. (2) represents unknown concentrations at a future timestep, where the right side of the equation represents known values at the current timestep. The surface chloride concentration and the time-dependent material properties (i.e., diffusion coefficient) of the concrete are calculated at the beginning (and held constant) during each timestep.

To numerically solve the diffusion equation, Eq. (2) can be rearranged into matrix form:

$$AU^{t+1} = BU^t (4)$$

where A and B are  $n \times n$  matrices corresponding to the dimensionless CFL number:

$$A = \begin{bmatrix} 1 & 0 & 0 \\ -r & 1+2r & -r & \cdots & 0 \\ 0 & -r & 1+2r & & & \vdots \\ & \vdots & & \ddots & & \vdots \\ & & & 1+2r & -r & 0 \\ 0 & & \cdots & -r & 1+2r & -r \\ & & & 0 & 0 & 1 \end{bmatrix}$$
 (5)

$$B = \begin{bmatrix} 1 & 0 & 0 \\ r & 1 - 2r & r & \cdots & 0 \\ 0 & r & 1 - 2r & & & \\ & \vdots & & \ddots & & \vdots \\ & & & 1 - 2r & r & 0 \\ 0 & & \cdots & r & 1 - 2r & r \\ & & & 0 & 0 & 1 \end{bmatrix}$$
(6)

Given that the chloride diffusivity of recycled aggregates (which primarily consist of old mortar) is not similar to the diffusivities of impermeable normal aggregates or new cement paste, the diffusion coefficients of recycled aggregates were modeled by setting the CFL number, r, in A and B that corresponded with the nodes representing the location of the recycled aggregates to a constant that more accurately represented the higher chloride diffusivity of recycled aggregates ( $D_a = 12.5 \pm 2.0 \times 10^{-12} \, \text{m}^2/\text{s}$ ). See Section 2.3 for a summary of modeling parameters.

The  $U^{t}$  matrix defines the chloride concentration of each node throughout the cover depth at the present timestep:

$$U^{t} = \begin{bmatrix} u_{1}^{t} \\ \vdots \\ u_{i}^{t} \\ \vdots \\ u_{r}^{t} \end{bmatrix}$$

$$(7)$$

The node  $u_1^{\rm t}$  corresponds with the chloride concentration at the surface of the concrete, which was set at the start of each simulation and, subsequently, at the start of each iterative timestep according to the boundary condition models described in Section 2.1.5. Precontamination of recycled aggregates was modeled by setting initial chloride concentration of each node in  $U^{\rm t}$  that corresponded with the location of a randomly placed recycled aggregate equal to the degree of initial aggregate contamination (see Section 2.3). This procedure was performed only for the initial timestep, t=0, allowing the initial chloride contamination to diffuse through the bulk.

Using matrix inversion, Eq. (4) can be rearranged to solve for  $U^{t+1}$ , a matrix of chloride concentrations for each individual slice at the next timestep:

$$U^{t+1} = A^{-1}BU^{t} = \begin{bmatrix} u_{1}^{t+1} \\ \vdots \\ u_{i}^{t+1} \\ \vdots \\ u^{t+1} \end{bmatrix}$$
(8)

In the iterative numerical simulation, the  $U^{t+1}$  matrix thusly becomes the  $U^t$  matrix for the following timestep, and only the first term in the matrix need be updated to reflect the change in the surface boundary condition prior to stepping through the next iteration. See Section 2.1.5 for boundary condition modeling.

Since the Crank-Nicolson finite difference method accounts for both space and time, it is possible to included non-steady-state transport properties (e.g., chloride diffusion coefficients) and boundary conditions. Therefore, the effects of (1) *w/c* ratio, (2) SCMs, (3) time, and (4) temperature on the bulk apparent diffusion coefficient, (5) time-dependent boundary conditions, and the potential for (6) initial contamination of recycled aggregates were included in the modeling methodology. Mathematical incorporation of each of these effects is discussed in the following sections.

#### 2.1.1. Effect of w/c ratio

The w/c ratio is well known to impact chloride diffusion coefficients. Per the model proposed in [19], the effect of w/c ratio on the chloride diffusion coefficient was described by:

$$D_{28} = 2.17 \times 10^{-12} e^{\left(\frac{w/c}{0.279}\right)} \tag{9}$$

where  $D_{28}$  is the 28-day diffusion coefficient (m $^2$ /s), and w/c is in decimal form.

#### 2.1.2. Effect of SCMs

Previous research has shown that incorporating SCMs modifies many material properties of concrete, including chloride resistance. As proposed in [19,20], three SCMs, namely silica fume (SF), fly ash (FA), and metakaolin (MK), were considered to affect  $D_{28}$  according to:

$$D_{SF} = D_{28} \left[ 0.206 + 0.794 e^{\left( \frac{-SF}{2.51} \right)} \right] \tag{10}$$

$$D_{FA} = D_{28} \left[ 0.170 + 0.829 e^{\left( \frac{-FA}{6.07} \right)} \right] \tag{11}$$

$$D_{MK} = D_{28} \left[ 0.191 + 0.809 e^{\left( \frac{-MK}{6.12} \right)} \right] \tag{12}$$

where  $D_{\rm SF}$ ,  $D_{\rm FA}$ , and  $D_{\rm MK}$  are the modified 28-day diffusion coefficients due to the addition of *SF*, *FA*, and *MK*, respectively. *SF*, *FA*, and *MK* are the percent replacement (in whole-number percent) of ordinary Portland cement.

Additionally, two SCMs, namely FA and SG, alter the decay rate, m, of the diffusion coefficient when accounting for time (see Section 2.1.3) according to [19]:

$$m = 0.26 + 0.4 \left(\frac{FA}{50} + \frac{SG}{70}\right) \tag{13}$$

where FA and SG are again the whole-number percent replacement of ordinary portland cement by FA and SG, respectively.

SCMs also impact fresh-state workability, set time, and early strength gain of concrete when used in excessive amounts [21,22]. Thus, SCM additions in this model were limited to the replacement values listed in Table 1 that do not require corrective viscosity-modifying or set-accelerating admixtures.

**Table 1**Maximum replacement ratios of SCMs used in model implementation.

Allowable replacement of SCMs			
SCM	Max replacement	Source	
Silica fume	10%	[21,25]	
Fly ash	25%	[23,25]	
Metakaolin	20%	[22,24]	
Slag	50%	[26,27]	

#### 2.1.3. Effect of time

The chloride diffusion coefficient is a time-dependent parameter that is well known to decrease with time. This reduction is due, in part, to continued cement hydration and densification of the concrete beyond the first 28 days, among other mechanisms (i.e., carbonation). At each timestep, the bulk diffusivity was recalculated according to the following relationship:

$$D_{t}(t) = D_{28} \left(\frac{t_{28}}{t}\right)^{m} + D_{ult} \left(1 - \left(\frac{t_{28}}{t}\right)^{m}\right) \tag{14}$$

where  $D_{\rm t}$  is the time-dependent diffusion coefficient,  $D_{28}$  is either the 28-day diffusion coefficient calculated by Eq. (9) (without SCM addition) or Eqs. (10)(12) (with SCM addition), and the reference time,  $t_{28}$ , is typically taken as 28 days. As discussed, previous work [19] suggests that the chloride diffusion coefficient eventually plateaus to a final value. The second term of Eq. (14) accounts for this plateau effect via  $D_{\rm ult}$ , which is the 100-year ultimate diffusion coefficient calculated by the first term in Eq. (14).

#### 2.1.4. Effect of temperature

Temperature is an important consideration for a non-steadystate diffusion model as it can change the rate of concrete densification as well as the rate of chloride ion diffusion. To account for temperature-dependence of the chloride diffusion coefficient at each timestep, a simple Arrhenius relationship was implemented in this model [12]:

$$D_{dt,T}(t,T) = D_t(t) \cdot e^{\left[\frac{U_0}{R}\left(\frac{1}{\Gamma_r} - \frac{1}{T}\right)\right]}$$
 (15)

where  $D_{\rm t,T}$  is the time- and temperature-dependent diffusion coefficient (m²/s) at every node at each timestep throughout the cover depth, since temperature equilibrium was assumed to be reached immediately in comparison to chloride equilibrium,  $U_{\rm a}$  is the activation energy (J/mol), R is the universal gas constant (8.3144 J/mol/K), T is the average monthly temperature for the location of interest (K), and  $T_{\rm r}$  is the reference temperature equal to 20 °C (294.15 K).

#### 2.1.5. Chloride boundary condition modeling

Time-dependent chloride boundary conditions were modeled identically to the bilinear ramp-up and plateau models implemented in Life-365™. The ramp-up phase simulates chloride build-up due to cycles of wetting and drying at the concrete surface [12]. The slope of the ramp-up and the subsequent plateau of the chloride concentration at the concrete surface depend on both geographic location and exposure classification. Table 2 sum-

 Table 2

 Parameters for boundary condition modeling [12].

Zone	Exposure classification	Chloride concentration		
		Ramp-up (years)	Maximum (wt%)	
I	Marine Splash Zone	1	0.8	
II	Marine Spray Zone	10	1	
III	Within 800 m of Coastline	15	0.6	
IV	Within 1.5 km of Coastline	30	0.6	
V	Parking Structure	200	0.8	

marizes the boundary condition modeling parameters used in this study for each of the five exposure classifications. Given their similar coastal geographies, the boundary condition modeling parameters were identical for all exposure classifications in both geographic locations investigated in this study, namely Los Angeles, California (CA) and Anchorage, Alaska (AK).

#### 2.2. Time to cracking

Time to cracking is defined as the time from corrosion initiation to stress-induced cracking of the concrete cover based on the time-dependent formation of oxidation products. Time to cracking was estimated using a model proposed by Liu and Weyers [28], which has been used in many studies to predict cracking in reinforced concrete structures in chloride-laden environments [29–31]. According to the model,  $t_{\rm c}$ , can be predicted according to:

$$t_c = \frac{\left(W_{crit}\right)^2}{2k_n} \tag{16}$$

where  $W_{crit}$  is the amount of corrosion products required to cause cracking and  $k_p$  is the rate of rust production.  $W_{crit}$  can be computed according to the following:

$$W_{crit} = \rho_r \left( \pi \left[ \frac{x_s f_t'}{E_{eff}} \left( \frac{a^2 + b^2}{b^2 - a^2} + v \right) + t_p \right] d_b + \frac{W_{st}}{\rho_s} \right)$$
(17)

where  $x_c$  is the concrete cover depth,  $\rho_r$  and  $\rho_s$  are the density of rust and steel, respectively,  $f_t$  is the tensile strength of concrete (MPa), v is Poisson's ratio,  $t_p$  is the thickness of the porous zone surrounding the steel reinforcement,  $d_b$  is the diameter of the reinforcement, and  $E_{\rm eff}$  (MPa) is the effective elastic modulus of concrete modified by a creep coefficient,  $\varphi$ :

$$E_{eff} = \frac{E}{1 + \varphi} \tag{18}$$

The variables a and b are the inner and outer diameter (mm) of an idealized concrete cylinder, respectively:

$$a = \frac{d_b + 2t_p}{2} \tag{19}$$

$$b = x_c + a \tag{20}$$

The amount of corroded steel,  $W_{\rm st}$ , is equal to  $W_{\rm st} = \alpha W_{\rm crit}$ , where  $\alpha$  is the ratio of the molecular weight of steel and the molecular weight of rust products. The values for  $\alpha$  depend on the type of corrosion products and typically vary between 0.523–0.622 [28]. Finally, the rate of rust production is described:

$$k_p = \alpha^{-1} d_b i_{corr} \tag{21}$$

where  $i_{corr}$  is the annual mean corrosion rate (A/m<sup>2</sup>).

#### 2.3. Modeling parameters

Modeling parameters used in all numerical simulations are presented in Table 3. Means and standard deviations of all physical-based parameters were identified from lab or field measurements reported in literature.

Case study structures in two geographic locations were considered in this analysis. For each zone and location, four parameters (see Table 4) were varied to investigate the effects each had on the expected service life of recycled aggregate concrete. Initially, a default value for each of the four parameters was set as a baseline that was chosen to be representative of intermediate conditions or values that would be common in practice. Systematic analyses were conducted by varying a single parameter per simulation while holding the rest to default values.

**Table 3**Fixed modeling parameters. Deterministic parameters are shown as single values. Statistically distributed parameters are presented with a mean ± standard deviation.

Service-life modeling parameter	Value	Units	References
Time-to-corrosion-initiation			
Cover Thickness, $x_c$	70 ± 5	mm	[32,33]
Recycled aggregate diffusion coefficient, $D_a$	12.5 ± 2.0	kg/m <sup>3</sup>	[11,14]
Chloride threshold, $c_{\rm t}^{\rm a}$	$0.7 \pm 0.05$	kg/m <sup>3</sup>	[34-36]
Time to corrosion cracking			
Tensile strength, f't	$3.75 \pm 0.5$	MPa	[37]
Modulus of elasticity, E	$30 \pm 3.0$	GPa	[37]
Phi (creep coefficient), $\phi$	2	-	[28]
Poisson's ratio, v	0.18	-	[28,38]
Density of rust, $\rho_{\rm r}$	3600	kg/m <sup>3</sup>	[28,39]
Density of steel, $\rho_s$	7850	kg/m <sup>3</sup>	[28,39]
Thickness of porous region, $t_p$	$12.5 \pm 0.5$	μm	[28,40]
Corrosion rate, $i_{\rm corr}$	$2.5 \pm 0.5$	μA/cm³	[28,39]
Alpha, α <sup>b</sup>	0.523-0.622	-	[28]
Mild steel rebar diameter, $d_{\rm b}$	9.5	mm	

<sup>&</sup>lt;sup>a</sup> Lognormally distributed.

#### 2.4. Numerical simulation procedure

In the numerical simulation, first, geographic location and exposure zone were defined, which determined average monthly temperature profiles and parameters for the chloride boundary condition modeling (Table 2), respectively. This study explicitly investigated two locations, namely Los Angeles, CA and Anchorage, AK, whose average monthly temperature profiles are shown in Fig. 1.

Monte Carlo analysis was used to incorporate uncertainty to account for in-field variation in concrete cover depth, chloride threshold, and material properties via a simple bootstrap method similarly employed in [32] in which modeling parameters that were statistically distributed were first sampled from assumed distributions for each simulation. A normal distribution was assumed for all parameters unless otherwise noted. Therefore, once geographic location and zone were defined, the fixed time-tocorrosion-initiation modeling parameters (Table 3) were sampled from their respective statistical distributions, along with deterministic variables that were explicitly under investigation and directly defined by the user (Table 4). Aggregate placement was then randomly generated throughout the cover depth by (1) dividing the cover depth by maximum aggregate size into aggregate zones (to the nearest lower-bound integer) and (2) randomly placing an aggregate within each of those zones assuming a uniform distribution of placement while ensuring no aggregate overlap. A statistical test was used to designate aggregates as normal or recycled aggregates, according to the replacement ratio explicitly defined by the user (Table 3). As discussed in Section 2.1, the CFL number for recycled aggregates was fixed for the entire simulation for those nodes that corresponded to the placement of recycled aggregates. Else, the chloride diffusion coefficient was used for each node throughout the cover depth, including those nodes corresponding to normal aggregates, as similarly employed by Life-365™.

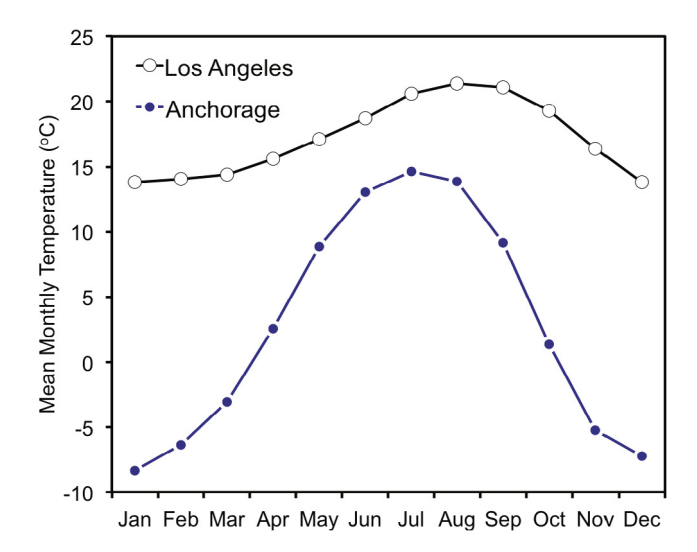


**Fig. 1.** Average monthly temperature profiles for Los Angeles, CA and Anchorage, AK [12].

The model then calculated the w/c- and SCM-modified baseline  $(D_{28})$  diffusion coefficient (Eqs. (9)(12)). At each subsequent timestep, a new time- and temperature-dependent chloride diffusion coefficient was determined according to Eqs. (14) and (15), respectively, and the new chloride distribution throughout the cover depth was calculated for the next timestep according to matrix inversion (Eq. (8)). Timesteps were taken to be one-month increments, and the cover was discretized into 300 equal slices (s = 300, n = 301). After each timestep, if the concentration at the cover depth was greater than or equal to the randomly generated chloride threshold from Table 3, corrosion initiation was assumed to have occurred for that simulation, and the model would store this time as time to corrosion initiation,  $t_i$ .

Once time to corrosion initiation was calculated, time to cracking,  $t_{\rm c}$  was computed directly using Eq. (16) with randomly sampled inputs from parameters listed in Table 3.

Each computed service life (total time to cracking),  $t_s = t_i + t_c$ , was then stored and the stochastic process was repeated. By an analysis of variance, a total of 20,000 Monte Carlo simulations were required to yield statistically significant predictions for expected service life of recycled aggregate concrete.

#### 3. Results and discussion

#### 3.1. Model validation

The proposed numerical model was validated via comparison with the Life-365<sup>M</sup> service life prediction software using normal aggregate concrete with the parameters listed in Table 5. Comparisons were made using deterministic values. For validation purposes, results were obtained for both a numerical model that employed an identical input for a constant decay factor (m = 0.2) that is used in the current version of Life-365<sup>M</sup> [12] (Numerical Model A) and the numerical model proposed herein (Numerical

 Table 4

 Variable modeling parameters. Default values were held constant in simulations where others were varied to elucidate effects on expected service-life of recycled aggregate concrete.

Parameters	Default values	Investigated values	Units	References
Water-to-Cement (w/c) Ratio	0.45	0.30 0.35 0.40 0.45	_	[41]
Aggregate pre-contamination	2.0	1.00 1.50 2.00 2.50	kg/m <sup>3</sup>	[42]
Aggregate diameter	9.5	9.50 12.7 19.0 25.4	mm	[43]
Aggregate replacement ratio	0.5	0.30 0.50 0.70 1.00	-	[41]

b Uniformly distributed.

**Table 5** Input parameters for model validation and comparison with Life-365™.

Thickness (mm)	Cover depth (mm)	Location	$D_{28} (\text{m}^2/\text{s})$	Chloride threshold (%)
500	70 mm	Los Angeles, CA	$1.1 \times 10^{-11}$	0.05

Model B) that included the most recent relationships for m (Eq. (13)), the diffusion coefficient plateau (Eq. (14)), and the effects of w/c and SCMs on  $D_{28}$ , as presented in Section 2.

The results of the model comparisons are shown in Table 6. The results substantiate that the numerical model was formulated identically to the numerical model used by Life- $365^{\mathbb{M}}$ . Minor differences ( $\leq 0.5\%$ ) between the results obtained by Numerical Model A and Life- $365^{\mathbb{M}}$  were determined to be a result of Life- $365^{\mathbb{M}}$  accounting for leap years. The differences between Numerical Model B and Life- $365^{\mathbb{M}}$  are attributable to the updated mathematical relationships for m and chloride diffusion coefficients, which are, incidentally, less conservative than the equations used in the current version of Life- $365^{\mathbb{M}}$ . Thus, the results obtained using Numerical Model B were used for the remainder of the analyses presented in this work.

#### 3.2. Impact of climate

To establish a normal aggregate concrete baseline, the effect of climate, namely average monthly temperature, on time-to-cracking of normal aggregate concrete (w/c = 0.45) in all exposure classifications is elucidated by the results presented in Fig. 2. Averaged data correspond to a 50% likelihood of corrosion-induced cracking as determined by the stochastic approach implemented by the numerical simulation. For example, in Anchorage, AK in Zone IV, there is a 50% likelihood that normal aggregate concrete will exhibit corrosion-induced cracking in 30.2 years, while, in Los Angeles, CA there is an identical likelihood that cracking will occur in 19.9 years for normal aggregate concrete placed in the same zone.

As anticipated, both location and chloride exposure conditions affect the expected service life of reinforced concrete. The service life of identical normal aggregate concretes exposed to the same boundary conditions is longer in colder climates (AK) than in warmer climates (CA) due to expected high temperature-dependent increases in the chloride diffusion coefficient. Similarly, as expected, more aggressive chloride exposure conditions in Zones I and II result in a reduced anticipated service life of normal aggregate concrete in comparison to lower chloride exposure conditions of Zones III, IV, and V in both geographic locations.

The results also illustrate that temperature-related increases in expected service life are more pronounced as chloride exposure conditions worsen. For instance, concrete placed in Zone I in Anchorage, AK exhibits a 65% increase in expected service life compared to the same concrete placed in Zone I in Los Angeles, CA. This temperature-related benefit decreases to 44% in Zone 5 exposure conditions, suggesting a more significant role of average temperature in extending the service life of concrete placed in high-exposure conditions.

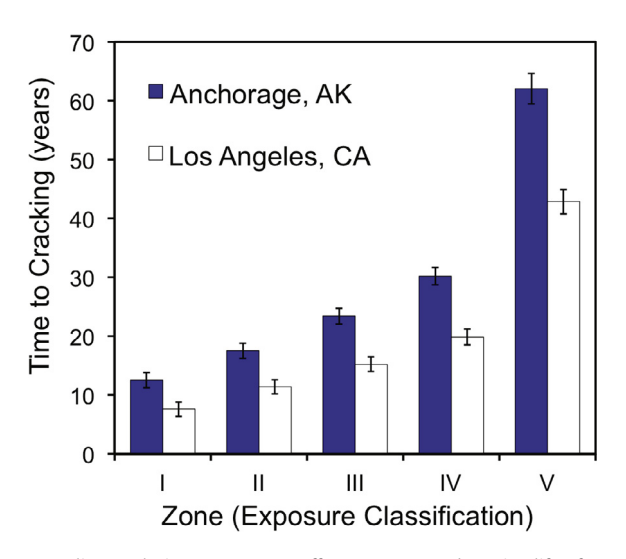


**Fig. 2.** Baseline analysis. Temperature effects on expected service life of normal aggregate concrete in five exposure classifications in Anchorage, AK and Los Angeles, CA.

#### 3.3. Impact of initial aggregate contamination

The effect of initial aggregate contamination on the service-life of recycled aggregate concrete in chloride-laden environments is shown in Fig. 3. The results were obtained from an analysis that used the default input parameters for recycled aggregate concrete listed in Table 4, namely a w/c = 0.45, aggregate replacement ratio of 0.5, and an aggregate diameter of 9.5 mm, and the initial aggregate contamination level was varied in the model by each of the incremental values in Table 4. Averaged data correspond to a 50% likelihood of corrosion-induced cracking as determined by the stochastic approach implemented by the numerical simulation.

As in previous work [11], the results indicate that, while all concretes exhibit reductions in service life from the normal aggregate baselines shown in Fig. 2, increases in initial aggregate contamination from 1.0 to 2.5 kg/m³ result in little variation in expected service life of recycled aggregate concrete. A 50% aggregate replacement and initial contamination decreased the service life by a maximum of 41% (in Los Angeles, CA) and a minimum of 23% (in Anchorage, AK) compared to the baseline case (Fig. 2) for the recycled aggregate concretes and ranges of initial aggregate contamination that were investigated in this study. Within each location and exposure condition, the difference between the lowest and highest contamination values decreased the expected service life by a maximum of 3.6% in Los Angeles, CA and 11.5% in Anchorage, AK, respectively. These results, however, were not statistically significant.

Table 6 Service-life prediction model validation and comparison with Life-365  $^{\rm TM}$ .

Zone	Life-365™ (Years)	Numerical Model A (Years)	% Difference	Numerical Model B (Years)
I	4.6	4.6	0.0%	5.8
II	8.6	8.6	0.0%	10.4
III	12.9	12.9	0.0%	15.7
IV	18.2	18.3	0.5%	22.1
V	45.1	45.3	0.4%	53

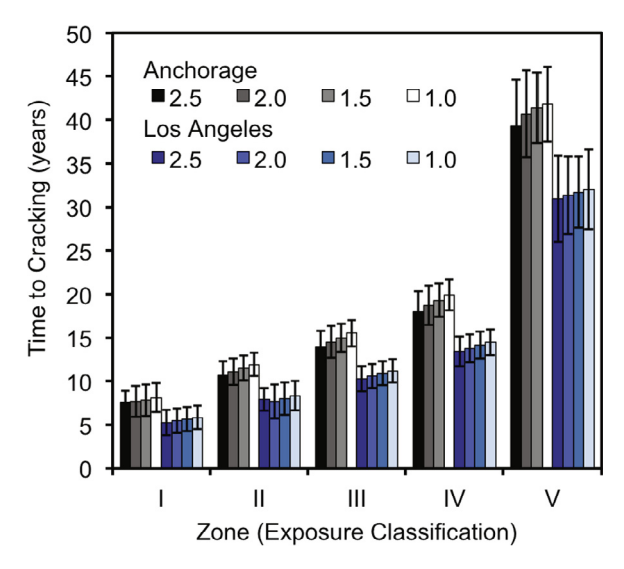


**Fig. 3.** Effect of initial aggregate contamination  $(kg/m^3)$  on expected service life of recycled aggregate concrete in five exposure classifications in Anchorage, AK and Los Angeles, CA.

While these results are specific to a recycled aggregate concrete with a 50% aggregate replacement ratio, w/c ratio of 0.45, and 9.5 mm aggregate diameter, previous research has comprehensively shown that the effect of initial contamination is minor in comparison to location and exposure conditions. Srubar [11] found that the effect of aggregate pre-contamination on expected time to cracking was less exaggerated in the presence of more aggressive external chlorides. These results also ascertain that external boundary conditions have a greater effect on in-service durability than does residual aggregate chloride contamination. Such findings suggest that certain levels of aggregate chloride contamination may be permissible in the design of recycled aggregate concrete structures in chloride-laden environments.

#### 3.4. Impact of recycled aggregate size

The effect of aggregate size on the anticipated service-life of recycled aggregate concrete is shown in Fig. 4. The results were obtained from an analysis that used the default input parameters for recycled aggregate concrete listed in Table 4, including an aggregate replacement ratio of 50% and an initial aggregate contamination of 2.0 kg/m³, which was assumed to ensure that approximately the same number and type of contaminated aggregate would be in each simulation. Aggregate diameter was varied in the model by each of the incremental values listed in Table 4. Averaged data correspond to a 50% likelihood of corrosion-induced cracking as determined by the stochastic approach implemented by the numerical simulation.

Similar to the effects of initial aggregate contamination, the results show that, despite initial reductions in expected service life compared to normal aggregate concrete, changes in aggregate diameter exhibit a negligible effect on the service life of contaminated recycled aggregate concrete. In contrast to the normal aggregate baseline case in Fig. 2, the expected service life of recycled aggregate concretes decreased by a maximum of 42% and a minimum of 25%. However, this reduction was uniform across all exposure classifications and ranges of aggregate diameter investigated herein. The slight increase in service life observed for the 19 mm aggregates is due to the partitioning of the cover depth in the numerical model and a maximum placement of three instead of four aggregates in series. These findings further suggest that aggregate size does not impart a significant effect on the durability of

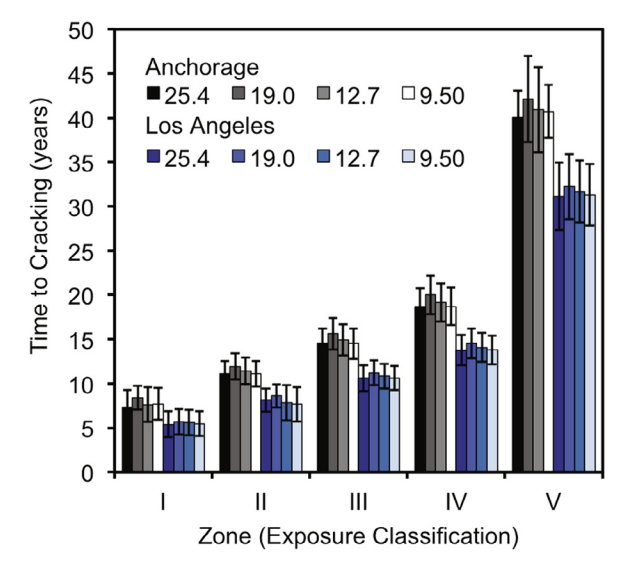


**Fig. 4.** Effect of aggregate diameter (mm) on expected service life of recycled aggregate concrete in five exposure classifications in Anchorage, AK and Los Angeles. CA.

recycled aggregate concrete structures., especially those in non-extreme chloride exposure conditions.

#### 3.5. Impact of recycled aggregate replacement ratio

The effect of aggregate replacement ratio on the anticipated service-life of recycled aggregate concrete is shown in Fig. 5. The results were obtained from an analysis that used the default input parameters for recycled aggregate concrete listed in Table 4, including an initial aggregate contamination level of 2.0 kg/m³. Aggregate replacement ratios were varied in the model from 30 to 100% by the incremental values listed in Table 4. A 0% replacement was not investigated, since such an analysis would correspond to the normal aggregate concrete baseline case presented in Fig. 2. Averaged data correspond to a 50% likelihood of corrosion-induced cracking as determined by the stochastic approach implemented by the numerical simulation.

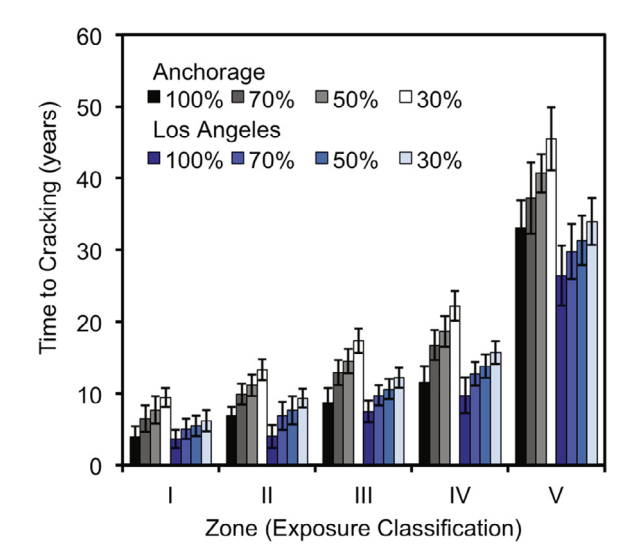


**Fig. 5.** Effect of recycled aggregate replacement ratio on expected service life of recycled aggregate concrete in five exposure classifications in Anchorage, AK and Los Angeles, CA.

As anticipated, the results show that an increase in aggregate replacement ratio decreases anticipated service life. Compared to the baseline case (Fig. 2), increasing the replacement ratio from 30% to 100% leads to a minimum and maximum reduction in expected service life of 18% (in Los Angeles, CA) and 68% (in Anchorage, AK), respectively. Within each exposure classification, the reductions are most pronounced in high-exposure conditions. For example, expected service life decreased 57% with increases in recycled aggregate replacement ratios from 30% to 100% in tidal zones (Zone I) in Anchorage, AK. In a low-exposure application (Zone V), expected service life of recycled aggregate concrete with identical recycled aggregate replacement ratios decreased only 22% in Los Angeles, CA.

Previous research on the effect of recycled aggregate replacement ratio on mechanical and durability properties of concrete has indicated that all levels of replacement are admissible, depending on the desired application, design life, and anticipated service life of recycled aggregate concrete [44,45]. The results from this analysis further substantiate this conclusion, given the range (6.2–45.5 years) of expected service life for recycled aggregate concrete. For some structural applications with design lives greater than 30 years, medium levels of pre-contamination (2.0 kg/m³) and high aggregate replacement ratios may be acceptable in some applications where mild levels of surface chloride exposure are anticipated. However, further analyses would need to be conducted to reveal absolute limits of aggregate replacement ratios and initial contamination given specific design scenarios in certain geographic locations.

#### 3.6. Impact of w/c ratio

Fig. 6 shows the effects of w/c ratio on the expected service life of recycled aggregate concrete. Results were obtained from an analysis that also used the default input parameters for recycled aggregate concrete listed in Table 4, including an aggregate replacement ratio of 50%, a constant aggregate diameter (9.5 mm), and an initial aggregate chloride contamination of  $2.0 \text{ kg/m}^3$ . For this analysis, the w/c ratio was varied in the model by the incremental values listed in Table 4 to elucidate the effects of w/c ratio on expected service life. Averaged data correspond to a 50% likelihood of corrosion-induced cracking as determined by the stochastic approach implemented by the numerical simulation.

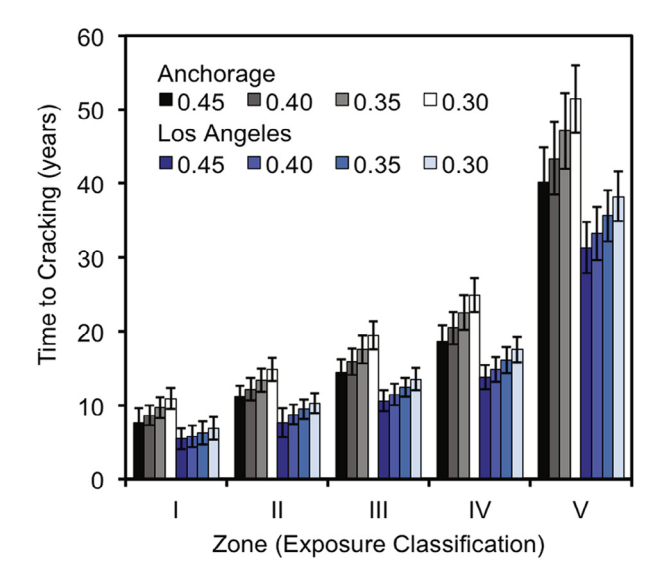


**Fig. 6.** Effect of *w/c* ratio expected service life of recycled aggregate concrete in five exposure classifications in Anchorage, AK and Los Angeles, CA.

As expected, an increase in *w/c* ratio results in a decrease in expected service life of recycled aggregate concrete in both locations across all exposure classifications investigated in this study. Increases in *w/c* ratio are well known to affect total porosity, chloride permeability, and, thus, expected service life of reinforced concrete in chloride-laden environments [5–7,10,46]. Increasing the *w/c* from 0.30 to 0.45 results in a minimum and maximum reduction in expected service life of 9% (in Los Angeles, CA) and 38% (in Anchorage, AK), respectively, in comparison to the normal aggregate concrete baseline case (see Fig. 2). This result can be attributed to even higher porosities and lower chloride resistances expected of recycled aggregate concrete in comparison to normal aggregate concrete.

Similar to increases in aggregate replacement ratio, the reductions in expected service life due to increases in *w/c* ratio are most pronounced in high-exposure environments. For instance, Fig. 6 illustrates that the expected service life of recycled aggregate concrete in Anchorage, AK decreases 29% and 22% in Zone I and Zone V, respectively, when *w/c* is varied from 0.30 to 0.45. Similar, yet less severe, reductions in Zone I (20%) and Zone V (18%) are observed for Los Angeles, CA. Together with the previously discussed results, these data suggest that, in addition to location, anticipated chloride exposure, and aggregate replacement ratio, *w/c* ratio remains an important durability parameter in estimating the service life of recycled aggregate concrete in chloride-laden environments.

#### 3.7. Impact of SCM additions

The effect of 5% SCM addition on the expected service life of recycled aggregate concrete is shown in Fig. 7. Results were obtained from an analysis that used the input parameters in the default case (DC) scenario for recycled aggregate concrete listed in Table 4, including a 50% recycled aggregate replacement ratio, initial aggregate contamination, a w/c = 0.45, and an aggregate diameter of 9.5 mm, and 0% SCMs. A fixed replacement of 5% for each SCM, namely fly ash (FA), slag (SG), silica fume (SF), and metakaolin (MK), was assumed for the comparative simulations and modeled according to the relationships presented in Section 2.1.2. The 5% cement replacement was chosen for illustrative purposes so that no SCM would be near its maximum advisable replacement limit set forth in Table 1. Averaged data correspond to a 50%

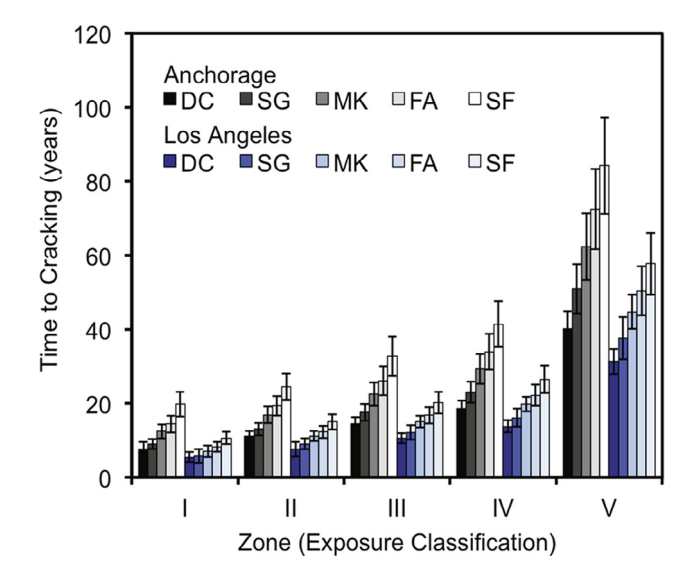


**Fig. 7.** Effect of 5% SCM replacement (by mass) on expected service life of recycled aggregate concrete in five exposure classifications in comparison to the default case (DC).

likelihood of corrosion-induced cracking as determined by the stochastic approach implemented by the numerical simulation.

The results in Fig. 7 reiterate that the inclusion of recycled aggregates in the default case scenario (DC) reduce chloride resistance and, subsequently, expected service life in contrast to normal aggregate concrete (Fig. 2). However, the results also indicate that additions of SCMs improve the performance of recycled aggregate concrete in chloride-laden environments compared to the recycled aggregate DC baseline. Extensive experimental research has previously shown that the inclusion of supplementary cementitious materials (SCMs) improves concrete mechanical properties and resistance to chloride ingress [19,47]. These modeling results also substantiate that SCMs would likely improve the expected service life of recycled aggregate concrete.

According to Fig. 7, even with a moderate replacement (5%) of ordinary portland cement, SCMs can overcome the initial reduction in service life that was expected of recycled aggregate concrete and, in some cases, supersede the service life of non-SCM normal aggregate concrete. For example, the expected service life of recycled aggregate concrete with 5% FA and 5% SF in Anchorage, AK exceeds that of normal aggregate concrete (Fig. 2) by 11–17% and 36–58%, respectively in Zones I-V. Similar, yet less substantial, increases in service life are observed for 5% replacements of FA and SF in all Zones in Los Angeles, CA.

The results also illustrate that SF and FA are more effective than metakaolin and slag in extending the anticipated service life of recycled aggregate concrete in small additions. This result can be attributed to high silica contents and, hence, increased pozzolanic reactivity of silica fume and fly ash in comparison to slag and metakaolin. The effect of the pozzolanic reaction, namely the reaction between soluble silica and calcium hydroxide that produces dense calcium-silicate-hydrate, on the bulk transport properties is taken into account in the modeling by modifying the effective diffusion coefficients calculated according to Eqs. (10)–(12).

In addition, the data suggest that benefits of 5% SCM additions on the expected service life of recycled aggregate concrete are both location- and application-dependent. With 157% and 96% increases in expected service life over the recycled aggregate concrete DC scenario, the use of 5% SF resulted in the most benefit in Zone I and Zone II applications in Anchorage, AK and Los Angeles, CA, respectively. The use of 5% FA, however, resulted in a maximum of 87% and 61% increase in expected service life over the recycled aggregate concrete DC scenario in Zone I and Zone IV applications in Anchorage, AK and Los Angeles, CA, respectively. Such results demonstrate the location- and application-dependencies of the effects that different SCMs would likely have on the expected service life of recycled aggregate concrete.

#### 3.8. SCM addition for 50-year service life

Previous experimental research has shown that the addition of SCMs in recycled aggregate concrete could result in concrete strength and durability performance equivalent to that of normal aggregate concrete [48,49]. However, the exact replacements needed for equal performance is uncertain due to the high variability in recycled aggregate quality and SCM chemistries investigated by these studies.

To better estimate required SCM replacements for equivalent service life performance, the data shown in Table 7 are the result of a hypothetical analysis that used the default input parameters for recycled aggregate concrete (DC) listed in Table 4 to investigate the type and quantity of SCMs required to reach a target 50-year design life in the five case-study applications in both Los Angeles, CA and Anchorage, AK. The model was implemented deterministically (i.e., no statistical sampling) utilizing a fixed aggregate position based on the specified aggregate replacement ratio (50%),

**Table 7**Hypothetical type and quantity of SCM (%) replacements needed to reach target 50-year service life in five exposure classifications in Anchorage, AK and Los Angeles, CA.

Zone	SF		FA		SG		MK	MK	
	AK	LA	AK	LA	AK	LA	AK	LA	
I	N/A	N/A	16	25	70	94	N/A	N/A	
II	N/A	N/A	14	23	61	75	N/A	N/A	
III	34	N/A	11	18	52	72	N/A	N/A	
IV	12	N/A	9	14	41	61	N/A	N/A	
V	1	3	3	7	6	21	5	26	

aggregate size (9.5 mm), degree of initial aggregate contamination (2.0 kg/m $^3$ ), and w/c ratio (0.45).

The data in Table 7 show the difference in performance among the four SCMs investigated herein. All values reported as N/A indicate that required SCM replacements exceeded 100% and were, thus, unattainable. The other values are hypothetical results that were not bound by the practical limitations listed in Table 1. Lower values required for identical applications in Anchorage, AK in comparison to Los Angeles, CA are again indicative of the effect of geographic location and elevated temperatures on exacerbating chloride diffusivity. Thus, higher SCM replacement percentages are required to meet the target design life for the same application in warmer climates.

The results suggest that FA and SG, not SF or MK, are most beneficial in increasing the expected service life of the recycled aggregate concrete DC scenario to 50 years, especially in high-exposure environments. According to the results, a replacement of 16% and 25% FA would reach a target design life of 50 years in Zone I exposure classifications in Anchorage, AK and Los Angeles, CA, respectively. Both replacement percentages of FA are well within the practical limits set forth in Table 1. Similarly, the percent replacements for SG are within reason, especially for Zone III-V exposure classifications in Anchorage, AK. Neither MK nor SF were as effective at improving the service life of the recycled aggregate concrete investigated in this particular analysis using the default parameters listed in Table 4. However, practical percent replacements of MK or SF could be achievable in extending the service life of other recycled aggregate concretes in high-exposure environments with different design parameters.

#### 4. Conclusions

This work presented the development, validation, and implementation of a 1D numerical service-life model for reinforced recycled aggregate concrete, which overcomes limitations of current service-life prediction models, including inabilities to account for fluctuating boundary conditions, time- and temperaturedependent chloride diffusion coefficients, and pre-contaminated recycled aggregates. Using a probabilistic approach, the model was first validated with the service-life prediction software Life-365™ and subsequently enhanced and employed to predict the time to corrosion-induced cracking of recycled aggregate concrete using aggregates (i) with and (ii) without initial chloride contamination from previous in-service exposure. Additionally, the impacts of location were investigated by temperature effects and variation of exposure conditions, namely structures located in a marine splash zone (Zone I), a marine spray zone (Zone II), within 800 km of coastline (Zone III), within 1.5 km of coastline (Zone IV) and parking structures (Zone V) in Los Angeles, California and Anchorage, Alaska. The effects of (a) degree of initial aggregate contamination, (b) aggregate size, (c) aggregate replacement ratio, and (d) water-to-cement (w/c) ratio were included in the model formulation, as were the effects of (e) supplementary cementitious materials (SCMs), namely fly ash, slag, silica fume, and metakaolin. The results from the subsequent analyses illustrate that, similar to normal aggregate concrete, exposure conditions, namely temperature and chloride exposure, exhibit the greatest impact on expected service life of recycled aggregate concrete. Results also show that increases in both aggregate replacement ratio and *w/c* ratio decrease expected service life. However, aggregate size and initial aggregate contamination levels were not found to affect expected service life in the applications and exposure conditions investigated herein. In regard to SCMs it was found that silica fume exhibited the most noticeable effect at low-percent replacements, while practical additions of fly ash and slag were the most viable in achieving a desired service life of 50 years in all five exposure cases for the recycled aggregate concrete investigated in this study.

The results indicate that moderate- to high-replacement ratios and some level of initial aggregate contamination may be permissible in the design of recycled aggregate concrete structures in chloride-laden environments and that the size of contaminated aggregates should not necessarily take priority as a durability design consideration. Analyzing the use of SCMs elucidated their importance, especially fly ash, if recycled aggregate concrete is to be used in applications with decades-long exposure to chlorides. Finally, the results indicate that recycled aggregate concrete appears to be best suited for cooler climates where service life can be prolonged simply through the retardation effect that lower temperatures have on chloride ingress.

#### Acknowledgments

This research was made possible by the Department of Civil, Environmental and Architectural Engineering, the College of Engineering and Applied Sciences, and the Sustainable Infrastructure Materials Laboratory (SIMLab) at the University of Colorado Boulder with partial support from the National Science Foundation (Award No. CMMI-1562557). The work presented in this study represents the views of the authors and not necessarily those of the sponsors.

#### References

- P.K. Mehta, P.J. Monterio, Concrete: Microstructure, Properties, and Materials, McGraw-Hill, NY, 2003.
- [2] J.D. Brito, N. Saikia, Recycled-aggregate in Concrete: Use of Industrial, Construction and Demolition Waste, Springer, London, 2013.
- [3] M. Malesev, V. Redonjanin, S. Marinkovic, Recycled concrete as aggregate for structural concrete production, Sustainability 2 (2010) 1204–1225.
- [4] M. Berndt, Properties of sustainable concrete containing fly ash, slag and recycled concrete aggregate, Constr. Build. Mater. 23 (2009) 2606–2613.
- [5] S.C. Kou, C.S. Poon, Compressive strength, pore size distribution and chlorideion penetration of recycled aggregate concrete incorporating Class-F fly ash, J. Wuhan Univ. Technol. – Mater. Sci. Ed. 21 (4) (2006) 130–136.
- [6] N. Otsuki, S. Miyazato, W. Yodsudjai, Influence of recycled aggregate on interfacial transition zone, strength, chloride penetration and carbonation of concrete, J. Mater. Civ. Eng. 5 (2003) 443–451.
- [7] H. Bo, L. Bing-kang, Z. Li-li, Chloride ion permeability test and analysis for recycled concrete, J. Hefei Univ. Technol. 32 (8) (2009) 1240–1243.
- [8] Y.A. Villagran-Zaccardi, C.J. Zega, A.A. Di Maio, Chloride penetration and binding in recycled concrete, J. Mater. Civ. Eng. 20 (6) (2008) 449–455.
   [9] R. Movassaghi, Durability of Reinforced Concrete Incorporating Recycled
- [9] R. Movassaghi, Durability of Reinforced Concrete Incorporating Recycled Concrete as Aggregate (RCA), U Waterloo Press, Waterloo, 2006.
- [10] F. Debieb, L. Courard, S. Kenai, R. Degeimbre, Mechanical and durability properties of concrete using contaminated recycled aggregates, Cem. Concr. Compos. 32 (2010) 421–426.
- [11] W.V. Srubar, Stochastic service-life modeling of chloride-induced corrosion in recycled-aggregate concrete, Cem. Concr. Compos. 55 (2015) 103–111.
- [12] Life-365 Consortium III. Life-365 service life prediction model and computer program for predicting the service life and life-cycle cost of reinforced concrete exposed to chlorides. 2014. Version 2.2.2.
- [13] K. Henchi, E. Samson, F. Chapdelaine, J. Marchand, Advanced finite-element predictive model for the service life prediction of concrete infrastructures in support of asset management and decision-making, Comput. Civ. Eng. (2007) 870–880.

- [14] J. Xiao, J. Ying, L. Shen, FEM simulation of chloride diffusion in modeled recycled aggregate concrete, Constr. Build. Mater. 29 (2012) 12–23.
- [15] J. Ying, J. Xiao, V.W. Tam, On the variability of chloride diffusion in modelled recycled aggregate concrete, Constr. Build. Mater. 41 (2013) 732–741.
- [16] K. Tuutti, Corrosion of steel in concrete: Report No. 4-82. Stockholm, Sweden: Swedish Cement and Concrete Research Institute, 1982.
- [17] K. Hong, R.D. Hooton, Effects of cyclic chloride exposure on penetration of concrete cover, Cem. Concr. Res. 29 (9) (1999) 1379–1386.
- [18] J. Crank, The Mathematics of Diffusion, Oxford UP, New York, 1975.
- [19] K.A. Riding, M.D.A. Thomas, K.J. Folliard, Apparent diffusivity model for concrete containing supplementary cementitious materials, ACI Mater. J. 110 (6) (2013) 705–714.
- [20] M.D.S. Thomas, P.B. Bamforth, Modelling chloride diffusion in concrete: effect of fly ash and slag, Cem. Concr. Res. 29 (4) (1999) 487–495.
- [21] R. Duval, E.H. Kadri, Influence of silica fume on the workability and the compressive strength of high-performance concretes', Concr. Res. 38 (4) (1998) 533–547.
- [22] S. Wild, J.M. Khatib, A. Jones, Relative strength, pozzolanic activity and cement hydration in superplasticized metakaolin concrete, Cem. Concr. Res. 26 (10) (1996) 1537–1544.
- [23] K. Obla, Specifying fly ash for use in concrete, Concr. Focus (2008) 60-66.
- [24] N. Ismael, M. Ghanim, Properties of blended cement using metakaolin and hydrated lime, Adv. Cem. Res. (2014) 1–8.
- [25] L. Lam, Y.L. Wong, C.S. Poon, Effect of fly ash and silica fume on compressive and fracture behaviors of concrete, Cem. Concr. Res. 28 (2) (1998) 271–283.
- [26] Portland Concrete Association (PCA). Fly ash, Silica Fume and Natural Pozzolans. Design and control of concrete mixtures, EB001, Ch. 3; p. 57–72.
- [27] C.M. Aldea, F. Young, K. Wang, S.P. Shah, Effects of curing conditions on properties of concrete using slag replacement, Cem. Concr. Res. 30 (2000) 465– 472.
- [28] T. Liu, R.W. Weyers, Modeling the dynamic corrosion process in chloride contaminated concrete structures, Cem. Concr. Res. 28 (3) (1998) 365–379.
- [29] T. El Maaddawy, K. Soudki, A model for prediction of time from corrosion initiation to corrosion cracking, Cem. Concr. Compos. 29 (3) (2007) 168–175.
- [30] D.V. Val, L. Chernin, Cover cracking in reinforced concrete elements due to corrosion, Struct. Infrastruct. Eng. 8 (6) (2012) 569–581.
- [31] I. Balafas, C.J. Burgoyne, Environmental effects on cover cracking due to corrosion, Cem. Concr. Res. 40 (9) (2010) 1429–1440.
- [32] T.J. Kirkpatrick, R.E. Weyers, C. Anderson-Cook, M.M. Sprinkel, M.C. Brown, A model to predict the impact of specification changes on chloride induced corrosion service life of Virginia bridge decks. Rep. No. VTRC03-CR4. VA Trans Res Council. 2003.
- [33] Y. Tanaka, H. Kawano, H. Watanabe, T. Nakajo, Study on cover depth for prestressed concrete bridges in airborne-chloride environments, PCI J. 51 (2) (2006) 42–53.
- [34] J. Zhang, Z. Lounis, Sensitivity analysis of simplified diffusion-based corrosion initiation model of concrete structures exposed to chlorides, Cem. Concr. Res. 36 (7) (2006) 1312–1323.
- [35] Z. Lounis, Uncertainty modeling of chloride contamination and corrosion of concrete bridges, in: Applied Research in Uncertainty Modeling and Analysis, Springer, US, 2005, pp. 491–511.
- [36] G.K. Glass, N.R. Buenfeld, The presentation of the chloride threshold level for corrosion of steel in concrete, Corros. Sci. 39 (5) (1997) 1001–1013.
- [37] S.C. Kou, C.S. Poon, Long-term mechanical and durability properties of recycled aggregate concrete prepared with the incorporation of fly ash, Cem. Concr. Compos. 37 (2013) 12–19.
- [38] C.Q. Li, Life-cycle modeling of corrosion-affected concrete structures: propagation, J. Struct. Eng. ASCE 129 (6) (2003) 753–761.
- [39] L. Qing, Reliability based service life prediction of corrosion affected concrete structures, J. Struct. Eng. – ASCE 130 (10) (2004) 1570–1577.
- [40] S. Care, Q.T. Nguyen, V. L'Hostis, Y. Berthaud, Mechanical properties of the rust layer induced by impressed current method in reinforced mortar, Cem. Concr. Res. 38 (8) (2008) 1079–1091.
- [41] M. Etxeberria, E. Vazquez, A. Mari, M. Barra, Influence of amount of recycled coarse aggregates and production process on properties of recycled aggregate concrete, Cem. Concr. Res. 37 (2007) 735–742.
- [42] F. Debieb, L. Courard, S. Kenai, R. Degeimbre, Roller compacted concrete with contaminated recycled aggregates, Constr. Build. Mater. 23 (2009) 3382–3387.
- [43] Portland Concrete Association (PCA). Aggregates for Concrete. Design and control of concrete mixtures, EB001, Ch. 5. pp. 79–103.
- [44] J. Xiao, J. Li, C. Zhang, Mechanical properties of recycled aggregate concrete
- under uniaxial loading, Cem. Concr. Res. 35 (6) (2005) 1187–1194. [45] S.M. Levy, P. Helene, Durability of recycled aggregates concrete: a safe way to
- sustainable development, Cem. Concr. Res. 34 (2005) 1975–1980. [46] S. Goto, D.M. Roy, The effect of w/c ratio and curing temperature on the permeability of hardened cement paste, Cem. Concr. Res. 11 (1981) 575–579.
- [47] V.G. Papadakis, Effect of supplementary cementing materials on concrete resistance against carbonation and chloride ingress, Cem. Concr. Res. 30 (2000) 291–299.
- [48] V. Corinaldesi, G. Moriconi, Influence of mineral additions on the performance of 100% recycled aggregate concrete, Constr. Build. Mater. 23 (2009) 2869–2876.
- [49] K.Y. Ann, H.Y. Moon, Y.B. Kim, J. Ryou, Durability of recycled aggregate concrete using pozzolanic materials, Waste Manage. 28 (2008) 993–999.